Available online at www.sciencedirect.com
SCIENCE DIRECT®
International Journal of Heat and Mass Transfer 47 (2004) 3491–3505
International Journal of HEAT and MASS TRANSFER
www.elsevier.com/locate/ijhmt

Some observations of the frost formation in free convection: with and without the presence of electric field

Chi-Chuan Wang [a,*], Ren-Tsung Huang [a,b], Wen-Jenn Sheu [b], Yu-Juei Chang [a]

[a] *Energy and Resources Laboratories, Industrial Technology Research Institute (ERL/ITRI), D400, Building 64, 195-6 Section 4, Chung Hsing Road, Hsinchu 310, Taiwan*

[b] *Department of Power Mechanical Engineering, National Tsing Hua University, Hsinchu 300, Taiwan*

Received 13 May 2003; received in revised form 7 January 2004
Available online 12 April 2004

Abstract

An experimental study concerning the frost formation in natural convection subjected to the influence of EHD is conducted. For the ambient temperature above the sub-freezing point and without the influence of EHD, water vapor deposited on the surface in the form of small droplets. A significant amount of coalescence of the small droplets is seen at the early stage of frost formation and the number of droplets increases with the relative humidity, but the size of the droplets decreases with the rise of the relative humidity. A hexagonal structure is observed as the droplet grew over a critical size ($d > 80$ μm). However, when the ambient temperature was below the sub-freezing temperature, the hexagonal structure was not seen because of the lack of droplets coalescence and the frost structure is comparatively uneven. With the presence of EHD, the ice column is pulled up towards the electrode and the structure is relatively skinny and fragile. The fragile structure can easily break up and fall off due to the influence of gravity. It was also found that the electric polarity plays a significant role on the frost growth. For a negative polarity, the frost structure is thinner than for a positive polarity and the break-off frequency of the ice column is more frequently compared to a positive polarity. It is likely that this phenomenon is related to the opposite direction of the dielectrophoreic force and the electrostrictive force at a positive polarity whereas the direction of the dielectrophoreic force and the electrostrictive force are the same at a negative polarity.

Keywords: Frost formation; Electrohydrodynamics; Electric polarity

1. Introduction

The adhesion of frost on the heat transfer surface is inevitable if the surface temperature is below the freezing point. Unfortunately, frost formation usually casts many negative effects upon the heat exchanger surfaces such as lower heat transfer coefficients, higher pressure drops, and system shutdown due to cycling defrosting.

There are many studies concerning the frost formation in natural convection having plate fin configurations. For example, Kennedy and Goodman [1] showed that a quasi-equilibrium state is reached for frost formation about 3 h, and the temperature of the air-frost interface approaches 0 °C. Moreover, the temperature of the air-frost interface oscillated around 0 °C. As the relative humidity is further increased, the period of these oscillations is shortened. Cremers and Mehra [2] reported that the frost-surface temperature was near or at the triple-point of water at a high relative humidity of 94%, while the value was slightly below the triple-point temperature at a low relative humidity of 53%. Fossa and Tanda [3] found that the deposited mass of frost is linearly increased with time, and the slope was considerably affected by the relative humidity of the ambient air, and is marginally affected by the temperature of the

* Corresponding author. Tel.: +886-3-5916294; fax: +886-3-5820250.
E-mail address: ccwang@itri.org.tw (C.-C. Wang).

0017-9310/$ - see front matter © 2004 Elsevier Ltd. All rights reserved.
doi:10.1016/j.ijheatmasstransfer.2003.12.021

Nomenclature

d	droplet diameter, m	T	temperature, °C
D	electric induction, $\mathrm{F\,V\,m^{-2}}$	T_d	dry bulb temperature, °C
E	electric field, $\mathrm{V\,m^{-1}}$	T_∞	ambient temperature, °C
f_b	electric body force, $\mathrm{N\,m^{-3}}$	V	supplied voltage, (V)
f_s	electrostrictive force, $\mathrm{N\,m^{-3}}$	z	distance from the surface, m
f_ε	dielectric force, $\mathrm{N\,m^{-3}}$	β	isobaric expansion coefficient, $\mathrm{K^{-1}}$
k	thermal conductivity, $\mathrm{W\,m^{-1}\,K^{-1}}$	ρ	density, $\mathrm{kg\,m^{-3}}$
RH	relative humidity	δ	frost thickness, mm
q	electric charge density, $\mathrm{C\,m^{-3}}$	ε	dielectric permittivity, $\mathrm{F\,m^{-1}}$
t	time, s		

cold plate. Schneider [4] proposed a correlation showing that the frost thickness was proportional to the square root of the elapsed time and to the temperature difference between the frost surface and the cold wall. Moreover, under the same relative humidity, the frost thickness was nearly independent of the ambient temperature. Hayashi et al. [5] classified three periods that characterize the frost formation process under free convection. Their classification is well recognized and accepted. For higher surface temperature and the lower relative humidity, Mao et al. [6] reported a smoother frost layer and the denser structure inside the frost layer.

Relative to the observations of frost formation in free convection, there were also many studies pertinent to the airside performance [7–13]. These results conclude that larger relative humidity will result in thicker frost layer and the corresponding heat transfer performance will deteriorate with elapsed time. In that regard, constantly defrosting of the heat transfer surface is required in order to make a thermal system functional. There are some possible methods to avoid frost formation in heat exchangers. The most common one is to constantly melt the frost either by turning off the cold airflow or by heating with an external heat source or with an internal hot gas by-pass refrigerant circuit. Apparently, many drawbacks are accompanied with this method, such as reduced equipment reliability, significant energy loss, and loss of operational load. There are also some passive methods such as employing hydrophilic coating on the heat transfer surface to reduce the frost formation [14,15]. However, based on the investigation by Wu and Webb [15], surface treatment will not help to reduce the frost formation but may be beneficial in defrosting cycle because condensate drainage can be easily achieved with hydrophilic coating.

In addition to the passive defrosting method, an active defrosting method that employs EHD (electrohydrodynamics) has received some attentions lately. Influence of EHD on frost formation was first reported by Schaefer [16] who showed a rapid growth of ice in the form of whisker-like aggregates in the presence of high electrical filed. Subsequently, Marshall and Gunn [17] observed a chaotic growth of ice showing many irregular branches on the ice crystals under the influence of weak electric fields. Bartlett et al. [18] discovered that frost immediately grew and stretched when the electric field strength was above 500 V/cm, and proposed that the ice crystals were destroyed because of the attracting force towards the electrodes. Maybank and Barthakur [19] conducted an experiment to see the effect of electric field on the ice crystal growth. Their results indicated a rapid growth of ice crystals when the applied electric field strength is above 200 V/cm. The observed crystals are thinner and more fragile as compared to those grown without electric field. Munakata et al. [20] utilized a mesh-like electrode design to suppress the frost formation on a cold plate. Their results indicated a 30% of reduction of frost at a supplied voltage of 7.5 kV. He also suggested that neither the hydrophilic nor the hydrophobic coatings of the surfaces can effectively reduce the frost formation under electric field. Libbrecht and Tanusheva [21] performed an experimental observation of the free dendrite growth of ice crystals from water vapor in supersaturated air. They reported a new type of dendrite growth instability by electrically enhanced diffusion of polar molecules at the dendrite tip. The nature of this external force demonstrated the growth instability which led to a rapid growth of ice needles with a tip velocity of approximately 5–50 times of the normal dendrite tip velocity without EHD. Blanford et al. [22] illustrated the influence of EHD on the frost formation with fin-and-tube heat exchangers. They found that frost formation decreased by 20% at low corona current (5 μA and less) but a 120% increase of frost formation was seen at high corona current (120 μA and more). Molki et al. [23] applied an intermittent electric field to suppress the amount of frost accumulation on a plate under natural convection. Unexpectedly, they found a rapid, avalanche-like destruction of the developed frost crystals under intermittent electric fields. Furthermore, they found that an intermittent electric field removed less frost than a continuous one in the

beginning but the situation is reversed after about one hour. Besides, higher frequency of the intermittence resulted in more effective removal of the frost.

The aforementioned studies provide some valuable information about the frost formation under electric field. However, the existing studies are still far from successfully implementing the EHD as a defrosting technique. Accordingly, it is the purpose of this study to reinforce this objective from fundamental visual observations. Efforts are focused on the influence of electric polarity.

2. Experimental setup

Experimental observations of the frost performance were conducted in an environmental chamber as shown in Fig. 1. The environmental chamber can control the ambient conditions in the range of $-10\ ^{\circ}\mathrm{C} \leqslant T_{\mathrm{d}} \leqslant 10\ ^{\circ}\mathrm{C}$ and $50\% \leqslant \mathrm{RH} \leqslant 90\%$. Controlled resolution for the dry bulb temperature is 0.3 °C while the controlled deviation of the inlet relative humidity at set point is 2%. The inlet and outlet relative humidities are measured by two humidity sensors with calibrated uncertainties of 2% (Delta 9861T). The schematic diagram of the experimental air circuit assembly is also shown in Fig. 1.

The test section consisted of an array of vertical surfaces which were aligned perpendicularly to the airflow direction. Detailed configurations of the extended surface were depicted in Fig. 2. The aluminum alloy 601 was chosen as the base and fin material because of its relatively high thermal conductivity and rigidity. The fin is 100 mm long, 100 mm wide, and 2 mm thick. The fins were mounted vertically on the aluminum alloy block as shown in Fig. 2. The base block was carefully machined to have 58 U-grooves. The width and height of the groove is 2 mm. It should be noticed that a high thermal conductivity grease ($k = 2.1\ \mathrm{W\,m^{-1}\,K^{-1}}$) was used to connect the fin and the base material to minimize the contact resistance. A mean gap distance of 0.05 mm is assumed between the attached fin and the base aluminum block. Actual fin base temperatures were then corrected from the measured temperatures. To measure the fin temperature in both directions of transverse and longitudinal to the airflow, a total of 10 thermocouples were mounted on one of the fins. Detailed locations of the thermocouples were shown in Fig. 2. These 'T'-type thermocouples were pre-calibrated with a resolution of

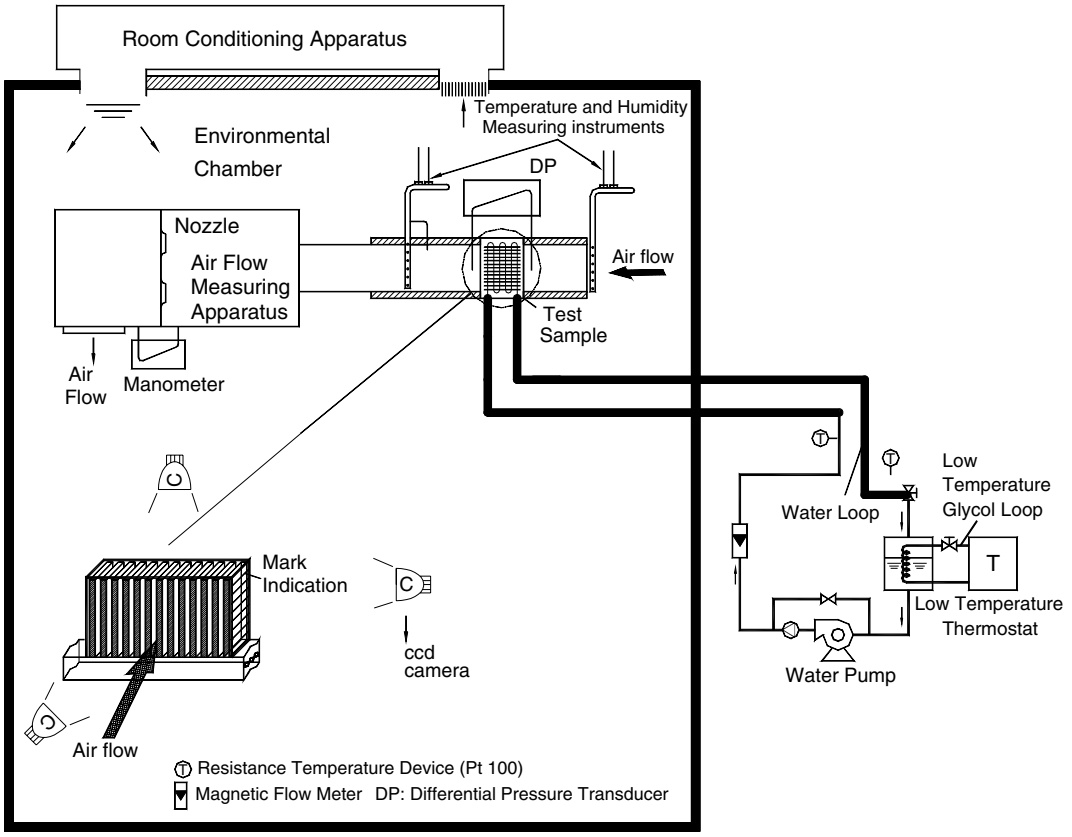

Fig. 1. Schematic of the test facility.

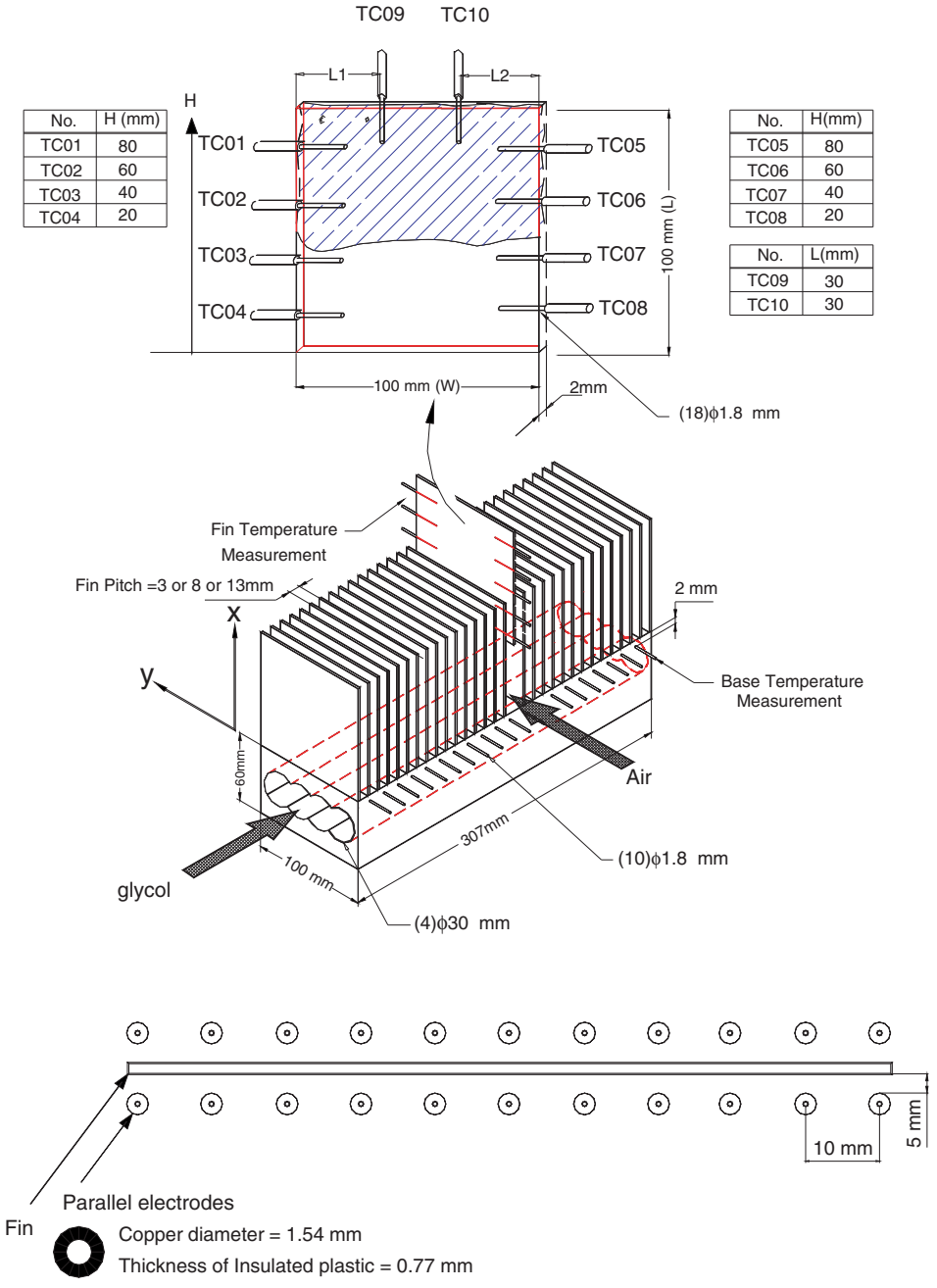

Fig. 2. Schematic of the test section and the location of the electrode.

0.1 °C. To heat up and cool down the fin array, water glycol was circulated via four drilled holes beneath the fin base of the aluminum block. A low temperature thermostat that is capable of providing water glycol at controlled temperatures of −10 to −20 °C. During the experiments, water glycol was circulated with a sufficiently high velocity (>1.0 m/s) to maintain the fin base temperature at a constant level. For various operation frontal velocities, the thermostat temperature was adjusted to keep the variation of the fin base temperature between inlet and outlet to be less than 0.3 °C. The test conditions are given as follows:

Ambient dry bulb temperature: −1 and 1 °C.
Ambient humidity: 60% and 80%.
Water glycol temperature at the inlet: −25 °C.

Base fin temperature: −20 °C.
Supplied DC voltage: −20, 10, 0, 10, and 20 kV.

Frost formulation on the fin was recorded by two CCD cameras which were placed above and in front of the fin surface. The image sensor is 1/4 in. image sensor having 410 K pixels with a scanning system of 525 lines and 60 fields/s. The lenses of the side-view and front view are Leica P/N 311383 and OLYMPUS NeoDPlan 10X, respectively. As shown in Fig. 2, the electrode used in this study consisted of 22 parallel insulated wires. The diameter of the wire electrode is 1.54 mm with insulated thickness of 0.77 mm. The gap of the electrodes to the fin surface is 5 mm whereas the center-to-center distance between wire electrodes is 10 mm.

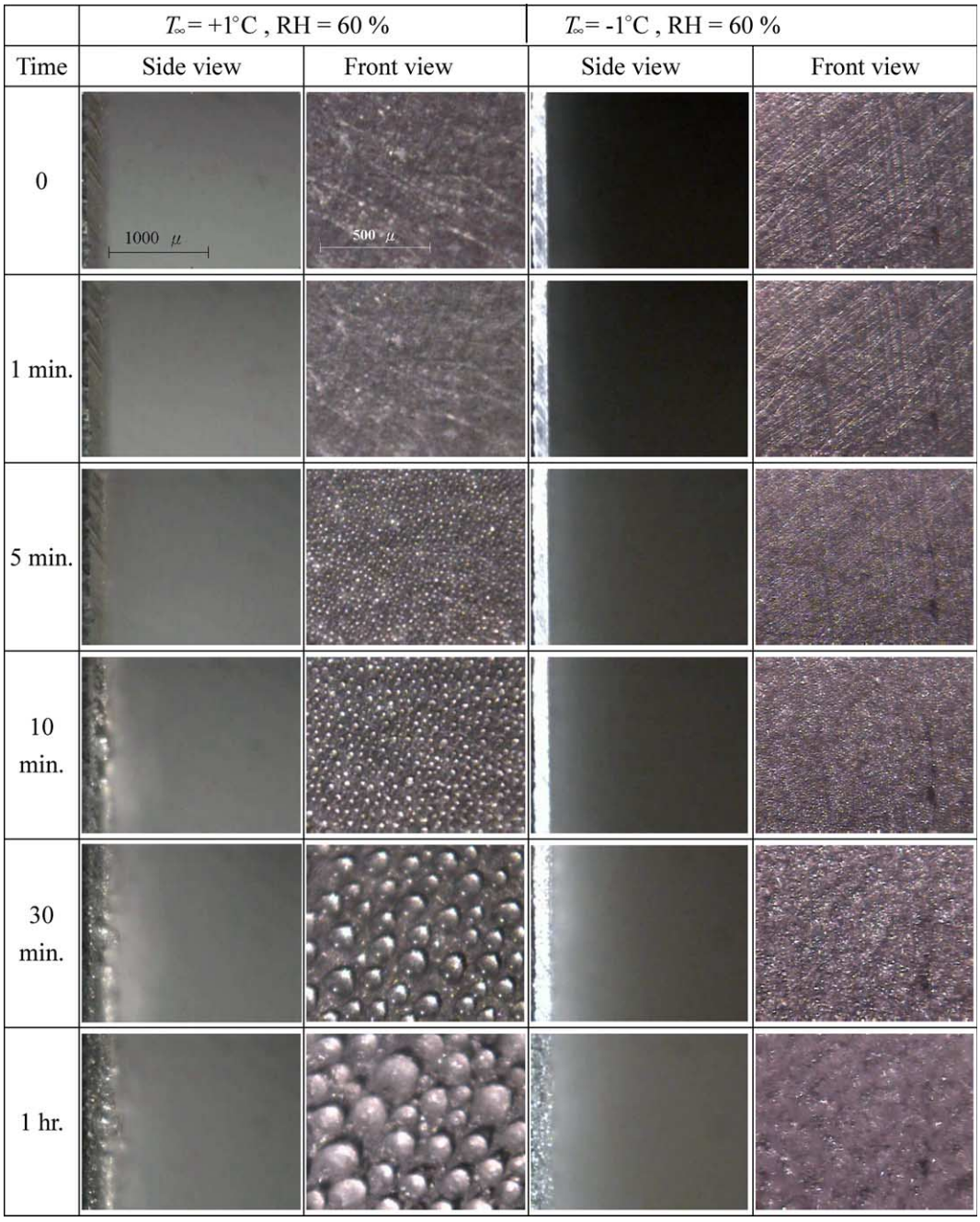

Fig. 3. Photos of the frost formation at $T_a = \pm 1$ °C and RH = 60% (without EHD).

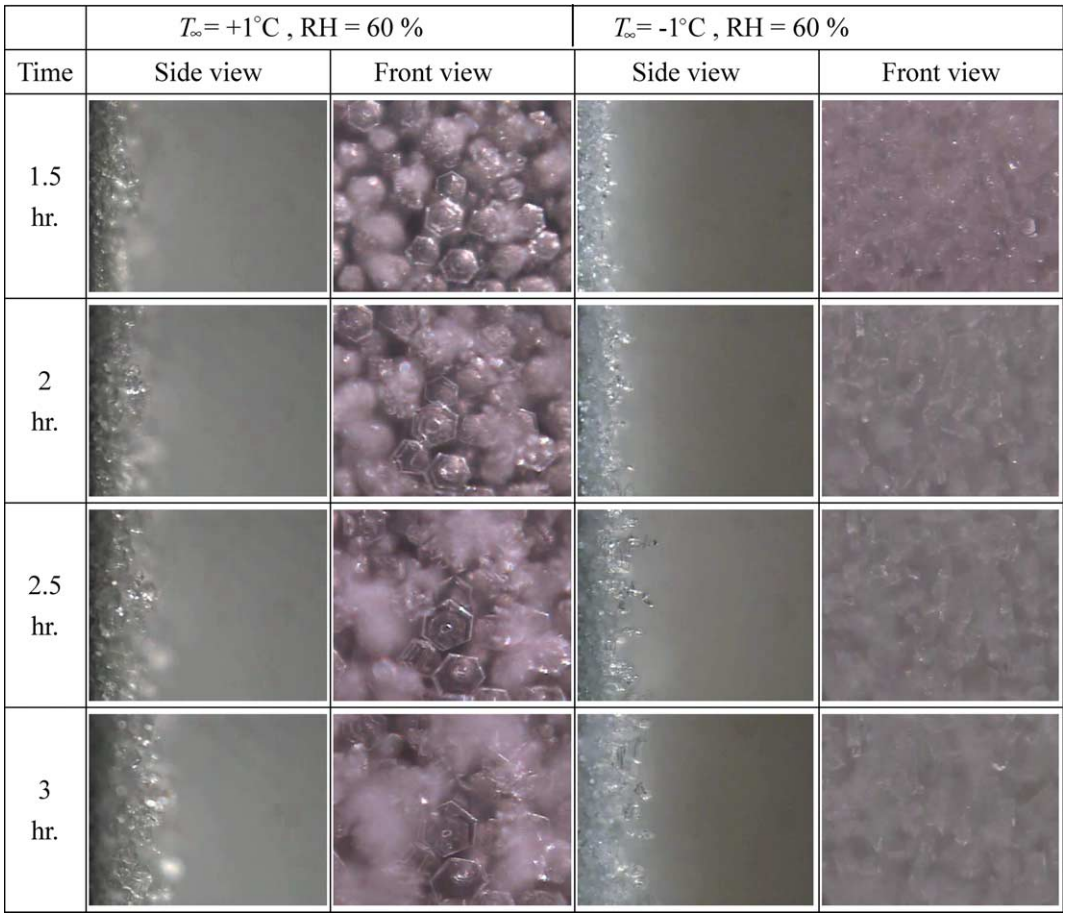

Fig. 3 (*continued*)

3. Results and discussion

Visual observations of the frost formation without the presence of EHD at $T_\infty = 1$ °C and −1 °C at $T_b = -20$ °C are schematically shown in Figs. 3 and 4. The relative humidity for Fig. 3 is 60% whereas is 80% for Fig. 4. The experiments were performed in a 3-h period. Notice that the sizes of the represented front-view and side-view in Figs. 3 and 4 are roughly 1 mm × 1 mm and 2 mm × 2 mm, respectively. More detailed length scale can also be seen in Fig. 3.

When the test is performed at a relative humidity of 60% at an ambient temperature of ±1 °C, as can be seen from the figure, for a period $t < 1$ min, there are hardly any noticeable changes in the surface. For $t = 5$ min, one can see very tiny condensate having hemisphere configuration forming on the surface at an ambient temperature of 1 °C. The small droplets then grew up by mutual coalescences. All the droplets then froze abruptly near an elapsed time of 30 min. The suddenly frozen phenomenon is analogous to those reported by Seki et al. [24] who also indicated a sudden freezing of the droplet near $t = 30$ min. Once the frost is formed ($t > 30$ min), the coalescence phenomenon of the neighboring ice column is not seen. Instead, as the ice column grew in time up to a critical size (around 80 μm), the neighboring frozen frost may encounter with each other. Consequently, converse to those small droplets showing coalescence phenomenon, the formed ice columns will squeeze with each other instead of merging into a bigger one. As a consequence, the squeezed frost changes its hemisphere shape to hexagon. Once the hexagonal ice column is formed, the free void space for the airflow to move around the ice column is considerably reduced. The water vapor diffusion inside the voids can no longer take place. A resultant transparent ice layer is formed on top of the hexagonal structure because of the subsequent melting and refreezing of the water condensate.

In contrast to the ambient temperature of 1 °C, at an ambient temperature of −1 °C that is below the sublimation temperature, the water vapor deposited on the surface in the form of frost and gradually grew in time.

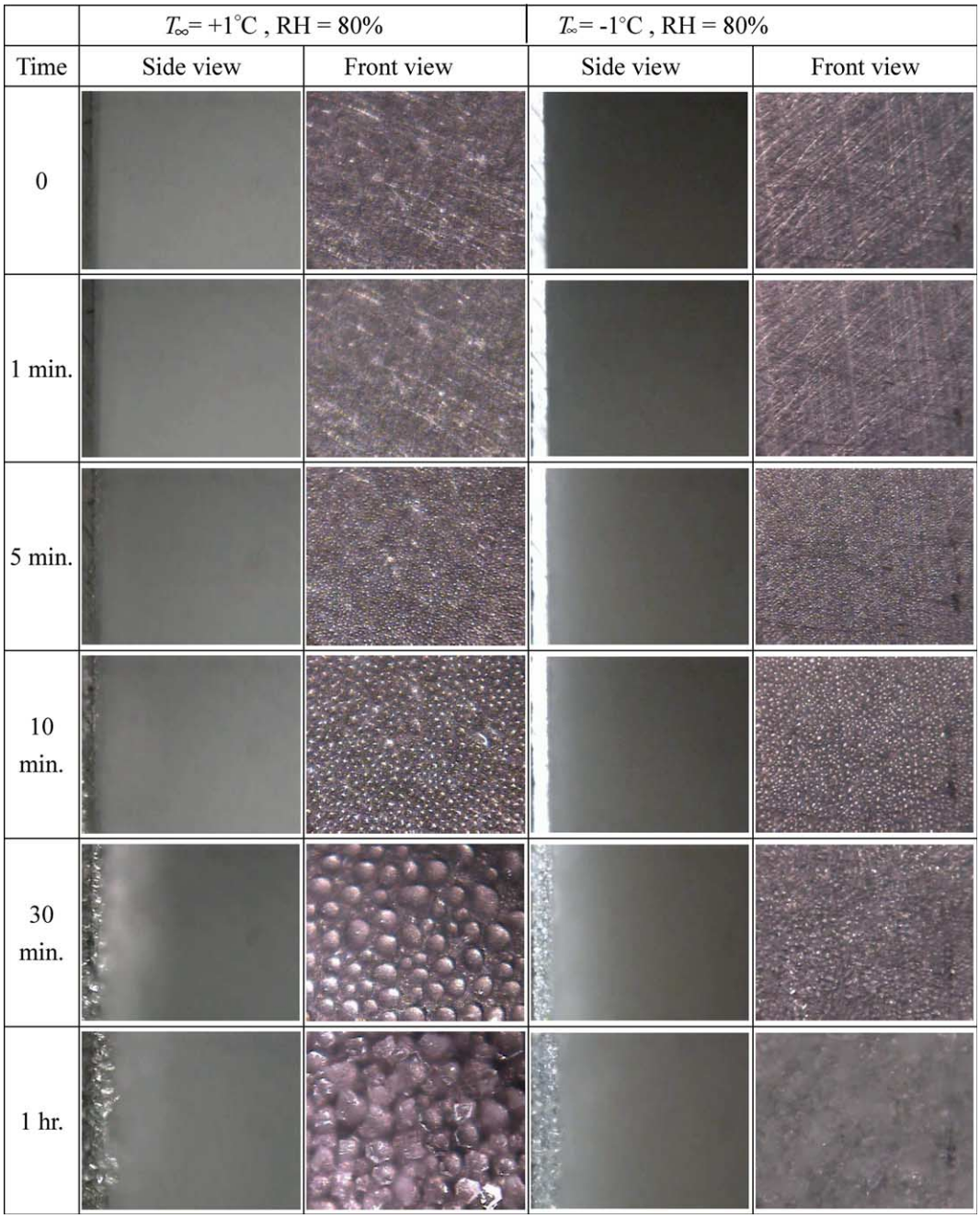

Fig. 4. Photos of the frost formation at $T_a = \pm 1$ °C and RH = 80% (without EHD).

Frost immediately formed on the surface instead of the super-cooled water condensate then freeze later as shown in Fig. 3. During the experimental period, neither droplet condensation nor coalescence of the neighboring droplet in a form of hemisphere at the early stage of frost formation is seen at an ambient temperature of −1 °C. As clearly shown in Fig. 4, the water vapor leaving air will pass directly from gaseous to solid state forming a porous layer. This layer will in turn cool down the air adjacent to it. At the early stage of frost formation, unlike small droplets showing a "wash of surface phenomenon" as they coalescence with one another, some of the water vapor will penetrate the frost thickness and diffuse and freeze at the surface. Therefore one can see a very thin white layer covering the surface. Basically, the frost formation is analogous to the description of

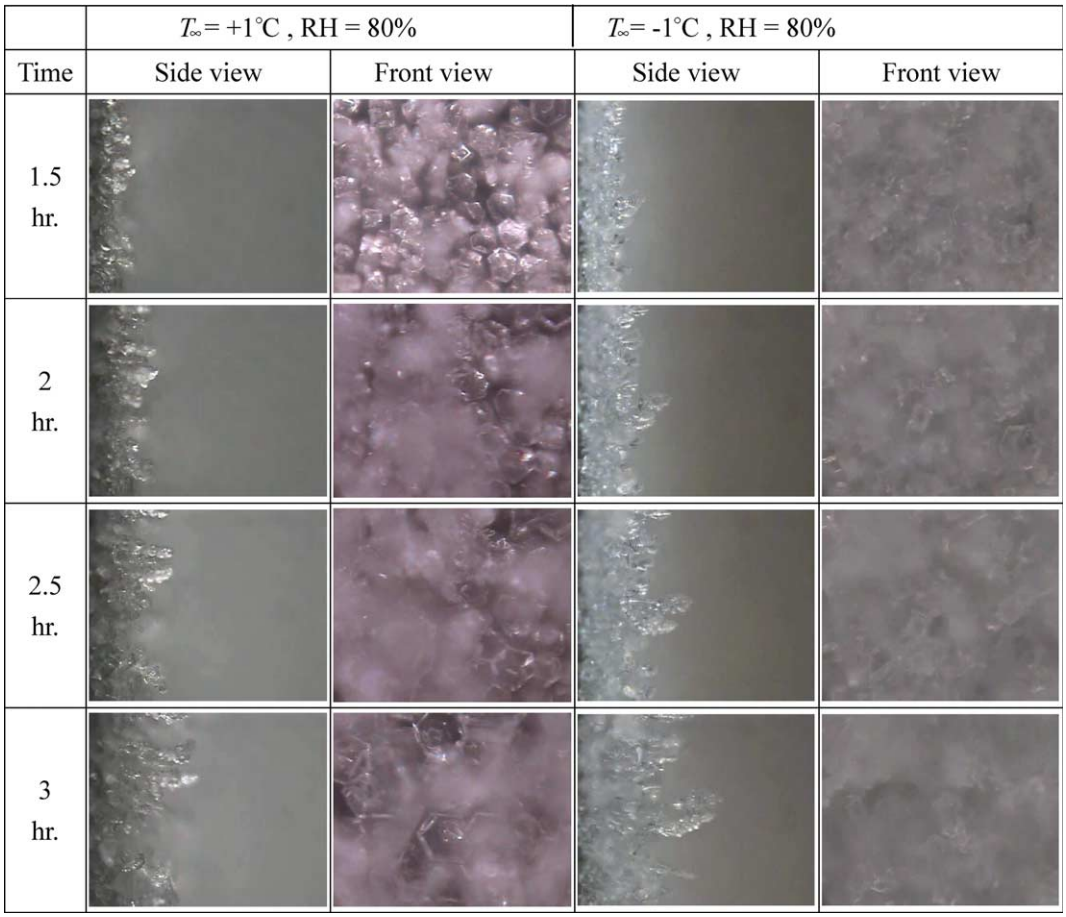

Fig. 4 (*continued*)

Hayashi et al. [5] who classified the frost formation into the crystal growth period, frost layer growth period, and frost layer full growth period. Examination of the frost crystal at the early stage ($t < 10$ min), the frost crystal grew mainly in one-dimension as that indicated by Hayashi et al. [5]. During the frost layer growth period, the frost structure changes from pure rod type into feather type crystal. The feather type crystal then grew into a very uneven surface condition at frost layer full growth period. Notice that the frost structure is still very robust irrespective of its unevenness.

As the ambient relative humidity is increased further to 80%, as shown in Fig. 4, the frost accumulation become more pronounced. For $T_\infty = 1$ °C, the number density of the droplets for RH = 80% is apparently higher than that of RH = 60% but the size of the droplet is comparably smaller for RH = 80%. Notice that the size of the droplet frost grew with time, yet the number density decreases considerably as it grew further. For instance, at RH = 80%, the number density exceeds 2500 per mm^2 at $t = 3$ min and the number density drops sharply to a number density of approximate 100 per mm^2 at $t = 20$ min whereas the mean droplet diameters grew from 10 to 70 μm.

With the presence of EHD of negative polarity of −5, −10, and −15 kV at $T_\infty = -1$ °C, visual results for RH = 80% vs. t are shown in Fig. 5. At the initial stage of frost formation ($t < 2$ min), there was no great distinction between those with and without EHD. As time is further increased, one can see a considerable difference in the number density of frost for those with EHD. For instance, at $t = 5$ min and RH = 80%, the number density of the ice column with EHD is only about one third of those without EHD. However, the rate of the decrease in the number density for EHD is not so pronounced as those without EHD. With the presence of the electric field, the deposited water vapor aligns in the direction of the electric field. Therefore one can see the crystal structure showing a relative thin and weak structure. The fragile structure then is pulled towards the electrode. Converse to those without EHD showing a considerable robust configuration, significant amount

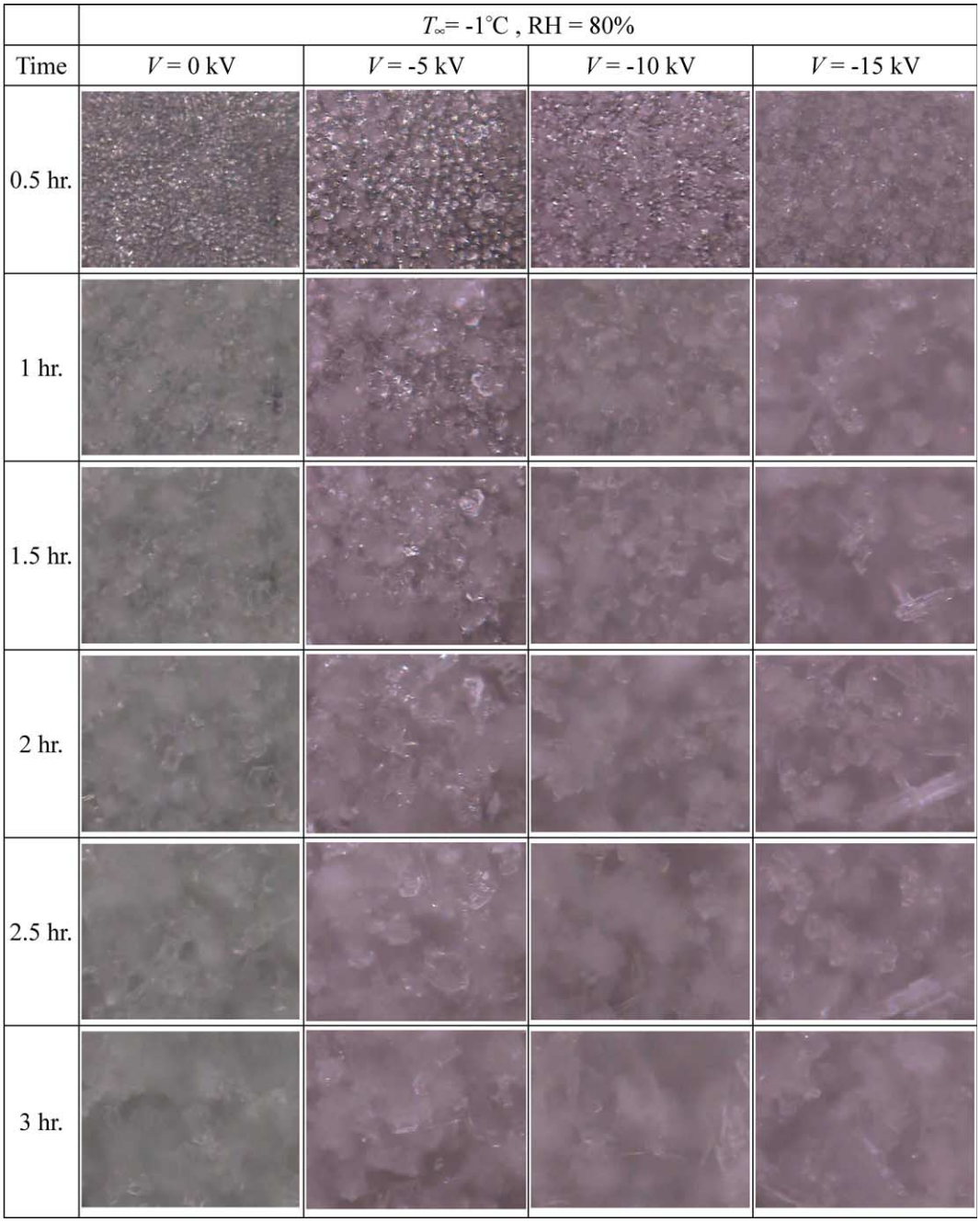

Fig. 5. (a) Photos of the frost formation at $T_a = -1$ °C and RH = 80% with negative polarity (front view). (b) Photos of the frost formation at $T_a = -1$ °C and RH = 80% with negative polarity (side view).

of the voids under the influence of EHD was seen. Therefore the water vapor diffusion inside the voids towards the surface is rather easy. This eventually leads to a better heat exchange of the air and the cold surface. As a consequence, the surface temperature with EHD is roughly 1–2° higher than that without EHD. With the presence of EHD, the smaller temperature difference between the cold surface and the free stream implies a higher heat transfer coefficient. In addition, because the frost structure is relatively irregular and rather thin, the frost structure may not sustain itself from gravity force as it grows further. Fig. 6 illustrates this break-off

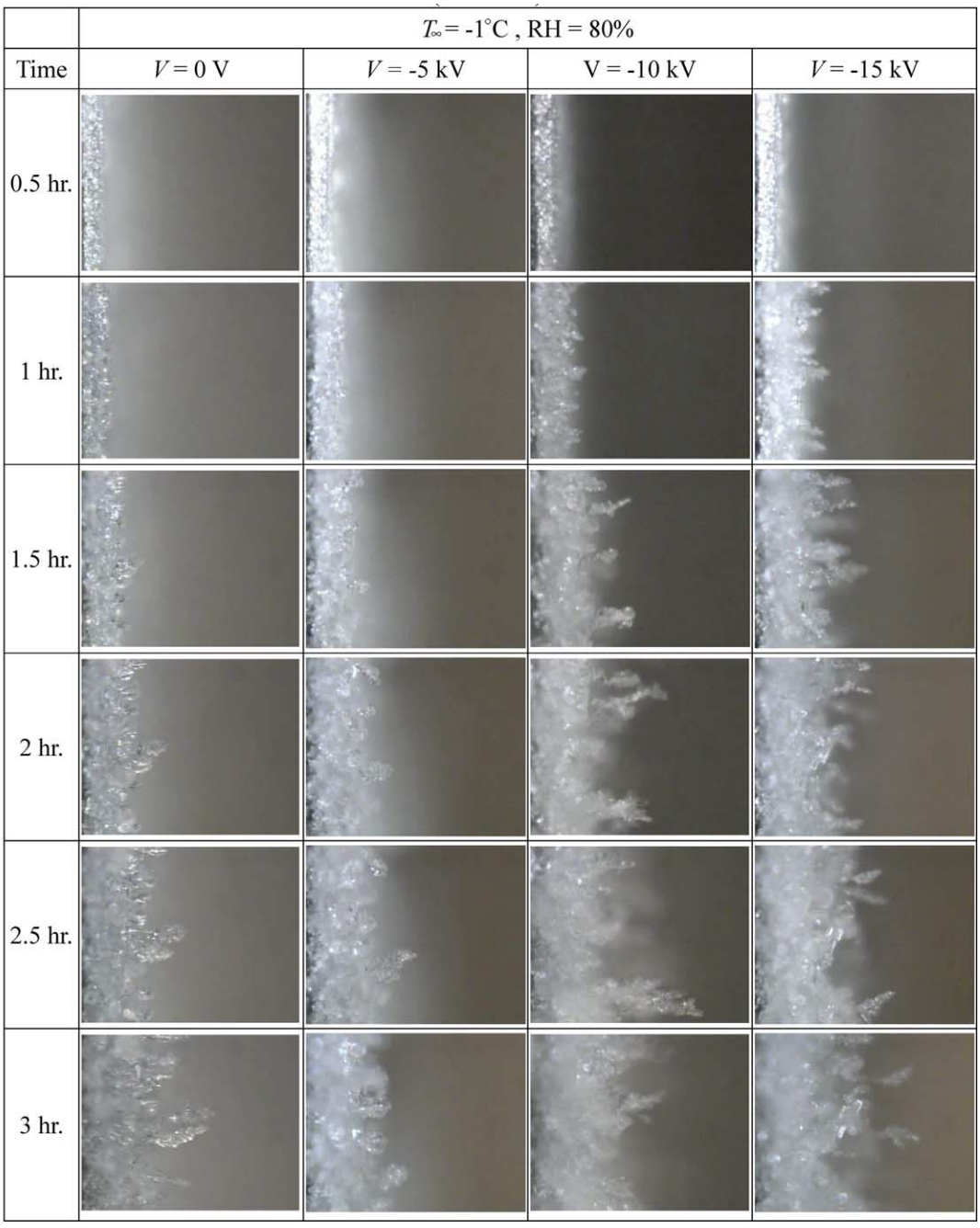

Fig. 5 (*continued*)

phenomenon under electric field. Notice that without the exerted force by the EHD ($V = 0$), the break-off phenomenon is not observed. The frequency of the break-off phenomenon increased with the strength of the applied electric field and with the increase of relative humidity.

In addition to the test performed at a negative polarity, visual results for positive polarity of +5, +10, and +15 kV are shown in Fig. 7. At first sight from the front view, the frost structure is similar to that of the negative polarity if the environmental conditions as well

Fig. 6. Schematic showing the break-off of the ice structure under electric field.

as the applied voltage are identical. However, as we look into the frost growth from the side view, one can clearly see the frost growth is comparatively inactive relative to that of the negative polarity. Despite the break-off phenomenon of the thin icy structure is still encountered, the frequency of the growth/break-off phenomenon is detectably smaller. Accordingly, one can see the maximum frost thickness under negative polarity is roughly 30–50% higher than that of the positive polarity as shown in Fig. 8. Explanations of this phenomenon can be borrowed the results from the theoretical/experimental study by Zaghdoudi and Lallemand [25] who performed pool boiling of *n*-pentane under the influence of DC electric polarity. As is well known, the electric forces within the dielectric fluid are given by

$$f_b = qE - \frac{1}{2}E^2\nabla\varepsilon + \frac{1}{2}E^2\nabla\left(\rho\frac{d\varepsilon}{d\rho}E^2\right). \quad (1)$$

The first term on the right-hand side of Eq. (1) is the Coulomb force exerted on the space electric charge in the dielectric fluid. The second term is the dielectrophoretic force f_ε that is due to spatial gradient of the dielectric permittivity and the third term is the electrostrictive force f_s caused by the variation of the dielectric permittivity as a function of the density and the non-uniformity of the electric field. By utilizing the temperature variations and the Clausius–Mossotti relation, the dielectrophoretic force f_ε and the electrostrictive force f_s can be expressed respectively as [25]:

$$f_\varepsilon = \frac{2(\varepsilon-\varepsilon_0)}{3\varepsilon}\left[-\left(\frac{\partial\varepsilon}{\partial T}\right)_\rho + \frac{\beta(\varepsilon-\varepsilon_0)(\varepsilon+2\varepsilon_0)}{3\varepsilon_0}\right] \times E^2\frac{dT}{dz}z, \quad (2)$$

$$f_s = \frac{(\varepsilon-\varepsilon_0)(\varepsilon+2\varepsilon_0)}{6\varepsilon_0\varepsilon^2}\frac{dD^2}{dz}z, \quad (3)$$

where D is the electric induction, β is the isobaric expansion coefficient, and the subscript 0 denotes the reference state. Since the permittivity decrease with the temperature, therefore the dielectrophoretic force f_ε is directed from the cooling surface towards the electrode. In the meanwhile, f_s is a function of the electric induction gradient and is related to the polarity of the applied electric field. For a negative polarity, the direction of f_s and f_ε is the same whereas the direction is opposite at a positive polarity [25]. Therefore, in a positive polarity, the resultant electric force is offset by the electrostrictive force f_s, thereby suppressing the pulled frost structure towards the electrode.

4. Conclusion

An experimental study concerning the frost formation in natural convection with the influence of EHD is conducted. Based on the present visualizations and measurements, the following conclusions are made:

(1) For an ambient temperature above the sub-freezing point and without the influence of EHD, water vapor deposited on the surface in the form of condensate droplets. A significant amount of coalescence of the small droplet is seen at the early stage of frost formation ($t < 30$ min). The number of droplets increases with the relative humidity but the size of the droplets decreases with the rise of the relative humidity. A hexagonal structure is observed as the droplet grew over a critical size ($d > 80$ μm). However, when the

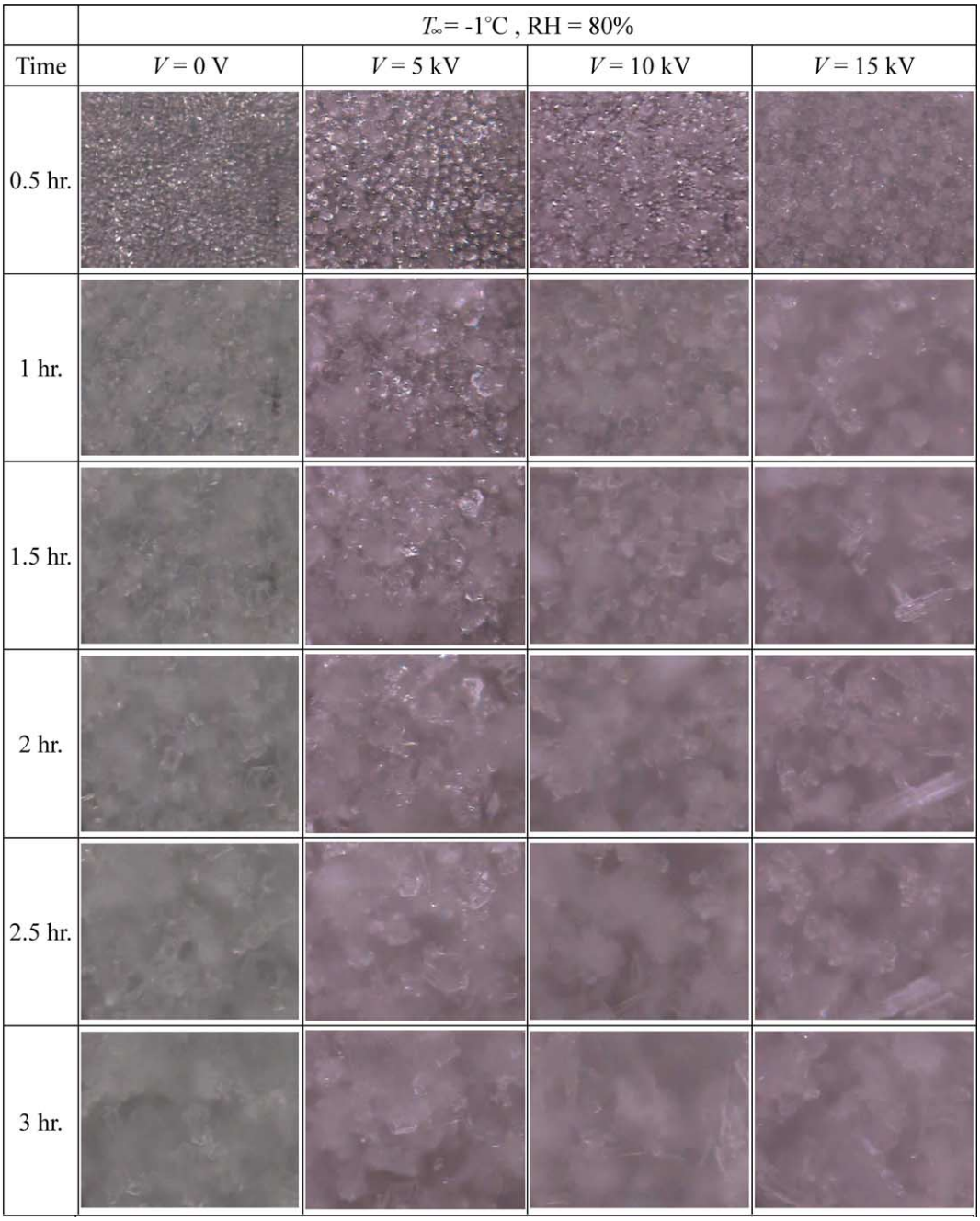

Fig. 7. (a) Photos of the frost formation at $T_a = -1$ °C and RH = 80% with positive polarity (front view). (b) Photos of the frost formation at $T_a = -1$ °C and RH = 80% with positive polarity (side view).

ambient temperature was below the sub-freezing temperature, the hexagonal structure was not seen because the lack of droplet condensation and coalescence. The frost structure at sub-freezing temperature is comparatively uneven.

(2) With the presence of EHD, the ice columns are pulled up towards the electrode. The frost structure has skinny and fragile shape and the weak structure can easily break up and fall off due to the influence of gravity.

(3) It is found that the speed of the frost growth and the break-off frequency of the ice column under negative polarity is roughly 30–50% higher than those with the positive polarity. It is likely that this

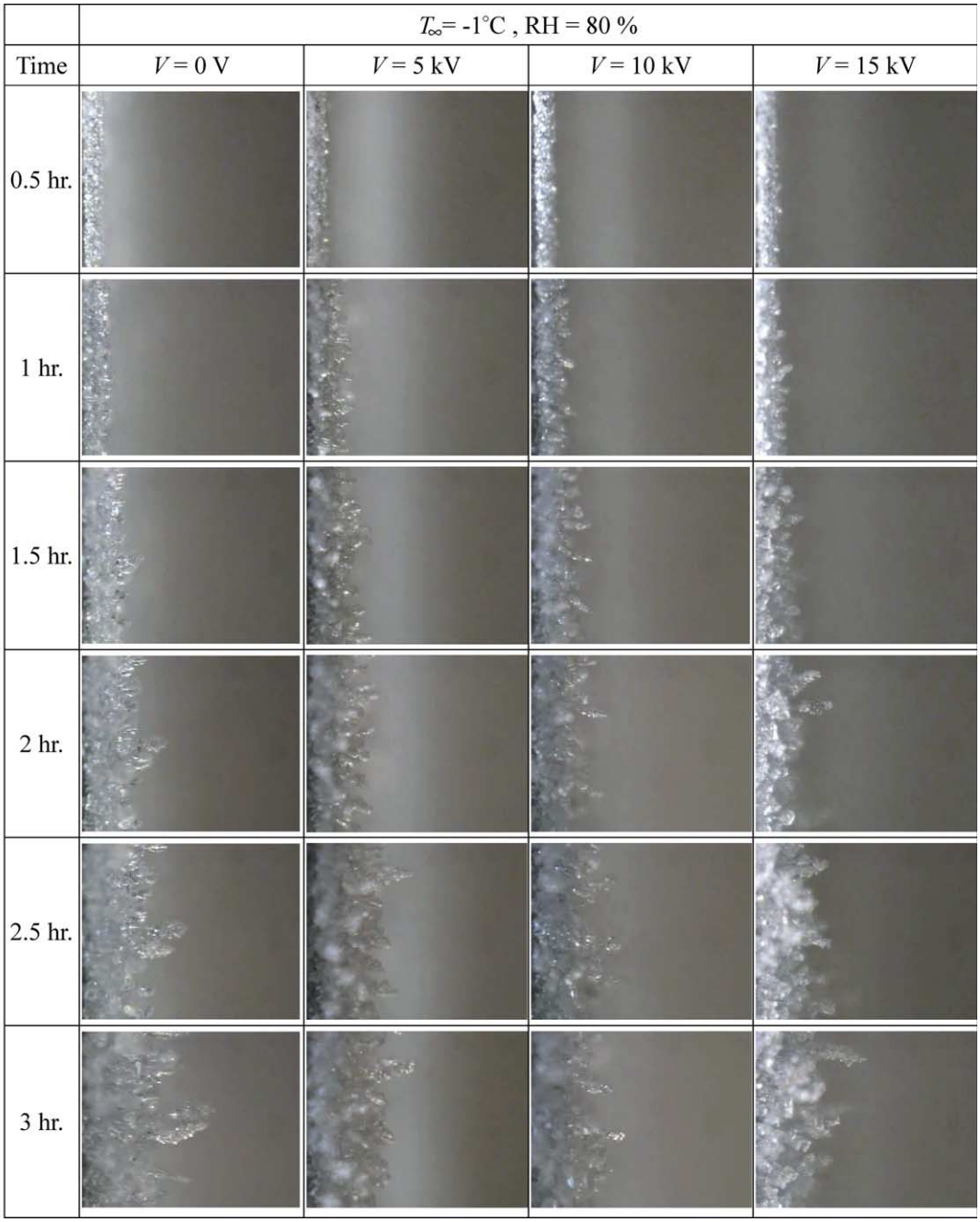

Fig. 7 (*continued*)

phenomenon is related to the opposite direction of the dielectrophoretic force and the electrostrictive force at a positive polarity whereas the direction of the dielectrophoretic force and the electrostrictive force are the same at a negative polarity.

Acknowledgements

The authors are indebted to the Energy R&D foundation funding from the Energy Commission of the Ministry of Economic Affairs and the research grant from National Science Council, Taiwan, R.O.C. under

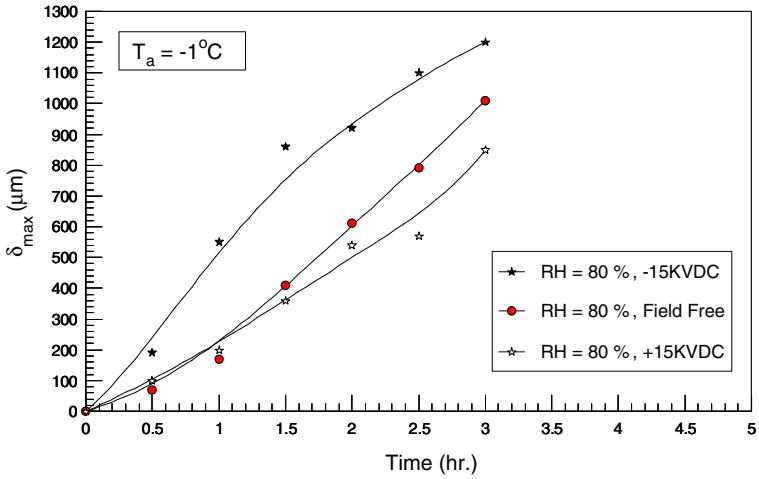

Fig. 8. Maximum frost thickness vs. time under the influence of electric polarity.

Grant NSC 91-ET-7-007-002-ET for supporting this study.

References

[1] L.A. Kennedy, J. Goodman, Free convection heat and mass transfer under conditions of frost deposition, Int. J. Heat Mass Transfer 17 (1973) 477–484.
[2] C.J. Cremers, V.K. Mehra, Frost formation on vertical cylinders in free convection, J. Heat Transfer 104 (1982) 3–7.
[3] M. Fossa, G. Tanda, Study of free convection frost formation on a vertical plate, Exp. Thermal Fluid Sci. 26 (2002) 661–668.
[4] H.W. Schneider, Equation of the growth rate of frost forming on cooled surface, Int. J. Heat Mass Transfer 21 (1978) 1019–1024.
[5] Y. Hayashi, A. Aoki, S. Adachi, K. Hori, Study of frost properties correlating with frost formation types, ASME J. Heat Transfer 99 (1977) 239–245.
[6] Y. Mao, R.W. Besant, K.S.J. Rezkallah, Measurement and correlations of frost properties with air flow over a flat plate, ASHRAE Trans. 98 (2) (1992) 65–78.
[7] C.A. Whitehurst, Heat and mass transfer to a metal plate by free convection from humid air under frosting conditions, ASHRAE J. 4 (1962) 58–69.
[8] O. Tajima, H. Yamada, Y. Kobayaashi, Y. Mizutani, Frost formation on air coolers part I: natural convection for a cooled plate facing upwards, Heat Transfer – Jpn. Res. 1 (2) (1971) 39–48.
[9] O. Tajima, E. Naito, Y. Tsutsumi, Y. Yoshida, Frost formation on air coolers part II: natural convection for a flat plate facing downwards, Heat Transfer – Jpn. Res. 3 (4) (1973) 55–66.
[10] O. Tajima, E. Naito, K. Nakashima, H. Yamamoto, Frost formation on air coolers part III: natural convection for a cooled vertical plate, Heat Transfer – Jpn. Res. 3 (4) (1974) 55–66.
[11] O. Tajima, E. Naito, T. Goto, S. Segawa, K. Nishimura, Frost formation on air coolers part IV: natural convection for two vertically opposed cooled plates, Heat Transfer – Jpn. Res. 4 (3) (1975) 21–36.
[12] R.F. Barron, L.S. Han, Heat and mass transfer to a cyro-surface in free convection, J. Heat Transfer 87 (1965) 499–506.
[13] N. Yamakawa, N. Takahashi, S. Ohtani, Forced convection heat and mass transfer under frost conditions, Heat Transfer – Jpn. Res. 1 (2) (1972) 1–10.
[14] E.U. Okoroafor, M. Newborough, Minimizing frost growth on cold surfaces exposed to humid air means of crosslinked hydrophilic polymeric coatings, Appl. Thermal Eng. 20 (2000) 737–758.
[15] X.M. Wu, R.L. Webb, Investigation of the possibility of frost release from a cold surface, Exp. Thermal Fluid Sci. 24 (2001) 151–156.
[16] V.J. Schaefer, Project Cirrus, Final Report, General Electric Research Laboratory, Schenectady, New York, 1950, p. 50.
[17] J.S. Marshall, K.L.S. Gunn, A first experiment on snow-crystal growth, in: H. Weickmann, W. Smith (Eds.), Artificial Simulation of Rain, Pergamon Press, New York, 1957, pp. 340–345.
[18] J.T. Bartlett, A.P. Van Den Heuval, B.J. Mason, The growth of ice crystals in an electric field, Z. Angew. Math. Phys. 14 (1963) 599–610.
[19] J. Maybank, N.N. Barthakur, Growth and destruction of ice filaments in an electric field, Nature 216 (1967) 50–52.
[20] T. Munakata, A. Yabe, I. Tanasawa, Effect of electric fields on frosting phenomenon, in: The 6th International Symposium on Transport Phenomena in Thermal Engineering, 1993, pp. 381–386.
[21] K.G. Libbrecht, V.M. Tanusheva, Cloud chambers and crystal growth: effects of electrically enhanced diffusion on dendrite formation from neutral molecules, Phys. Rev. E 59 (3) (1999) 3253–3261.
[22] M.D. Blanford, M.M. Ohadi, S.V. Dessiatoun, Compound air-side heat transfer enhancement in a cross-flow refrig-

erant-to-air heat exchanger, ASHRAE Trans. 101 (2) (1995) 1049–1054.

[23] M. Molki, M.M. Ohadi, M. Bloshteyn, Frost reduction under intermittent electric field, in: Proceedings of NHTC'00 34th National Heat Transfer Conference, Pittsburgh, PA, August 20–22, 2000.

[24] N. Seki, S. Fukusako, K. Matsuo, S. Uemra, An analysis of incipient frost formation, Wärme Stoffübertrag. 19 (1985) 9–18.

[25] M.C. Zaghdoudi, M. Lallemand, Analysis of the polarity influence on nucleate pool boiling under a DC electric field, ASME J. Heat Transfer 121 (1999) 856–864.